Animal Cells and Systems
Vol. 16, No. 5, October 2012, 376–384

Taylor & Francis
Taylor & Francis Group

The role of ginseng total saponin in transient receptor potential melastatin type 7 channels

Byung Joo Kim*

Division of Longevity and Biofunctional Medicine, Pusan National University, School of Korean Medicine, Beomeo-ri, Mulgeum-eup, Yangsan-si, Gyeongsangnam-do 626-870, Republic of Korea

(*Received 23 February 2012; received in revised form 19 March 2012; accepted 24 March 2012*)

Although ginsenosides have a variety of physiologic or pharmacologic functions in various regions, there are only a few reports on the effects of transient receptor potential melastatin 7 (TRPM7) channels. Here, we showed evidence suggesting that TRPM7 channels play an important role in ginseng total saponin (GTS)-mediated cellular injury. The combination techniques of electrophysiology, pharmacological analysis, small interfering RNA (siRNA) method and cell death assays were used. GTS depolarized the resting membrane potentials and decreased the amplitude of pacemaker potentials in cultured interstitial cells of Cajal (ICCs) in gastrointestinal (GI) tract. The TRPM7-like currents in single ICCs and the overexpressing TRPM7 in HEK293 cells were inhibited by GTS. However, GTS had no effect on Ca^{2+}-activated Cl^{-} conductance. GTS inhibited the survival of human gastric (AGS) and breast (MCF-7) adenocarcinoma cells. Also, GTS inhibited the TRPM7-like currents in AGS and MCF-7 cells. The GTS-mediated cytotoxicity was inhibited by TRPM7-specific siRNA. In addition, we showed that overexpression of TRPM7 channels in HEK293 cells was inhibited by GTS. Thus, TRPM7 channels are involved in GTS-mediated cell death in AGS and MCF-7 cells, and these channels may represent a novel target for physiological disorders where GTS plays an important role.

Keywords: transient receptor potential melastatin 7; TRPM7; ginseng total saponin; AGS cells; MCF-7 cells; apoptosis

Introduction

Ginseng, the root of *Panax ginseng* C. A. MEYER, is a well-known folk medicine and has been used as a tonic agent. The main molecular components responsible for the action of ginseng are the ginsenosides, which are also known as ginseng saponins. Ginsenoside is one of the derivatives of the triterpenoid dammarane consisting of 30 carbon atoms (Nah 1997). Ginsenoside has a four-ring, steroid-like structure with sugar moieties attached, and about 30 different forms have been isolated and identified from the root of *P. ginseng*. Ginseng total saponin (GTS) has a role of modulation of ion channels. GTS attenuated the N-Methyl-D-Aspartate (NMDA) receptor-mediated currents, and ginsenoside Rg3 inhibited the NMDA receptor and the neurotoxicity that it mediates (Kim et al. 2002, 2004). GTS modulated L-type Ca^{2+} channels in sensory neurons (Rhim et al. 2002) and also significantly inhibits the increase in $[Ca^{2+}]_i$ mediated by L-type Ca^{2+} channels but not by N-type Ca^{2+} channels in cultured hippocampal neurons (Kim et al. 2002).

Transient receptor potential melastatin 7 (TRPM7) is a member of the large Transient Receptor Potential (TRP) channel superfamily expressed in almost every tissue and cell type (Clapham 2003). Increasing evidence suggests that activation of TRPM7 channels contributes to various physiological and pathophysiological processes (Schmitz et al. 2003; Jiang et al. 2007; Jin et al. 2008). Notably, we demonstrated that human gastric adenocarcinoma cells express TRPM7 channel and its presence is essential for cell survival (Kim et al. 2008). Also, TRPM7 channel could regulate the proliferation of human breast cancer cells (Guilbert et al. 2009). Despite these facts, it has not been established whether TRPM7 channels play a role in GTS-mediated cytotoxicity in AGS and MCF-7 cells. In this study, we examined the effect of GTS on the pacemaking activity in interstitial cells of Cajal (ICCs), the pacemaker cells in gastrointestinal (GI) tract and the potential role of TRPM7 channels in the survival of GTS-mediated AGS and MCF-7 cells. Our data suggest that GTS has an important role in the modulation of TRPM7 channels.

Materials and methods

Preparation of cells and cell cultures

Balb/c mice (8–13 days old) of either sex were anesthetized with ether and killed by cervical dislocation. The small intestines from 1 cm below the pyloric

*Corresponding author. Email: vision@pusan.ac.kr

ISSN 1976-8354 print/ISSN 2151-2485 online

http://dx.doi.org/10.1080/19768354.2012.680495
http://www.tandfonline.com

ring to the cecum were removed and opened along the mesenteric border. The luminal contents were washed out with Krebs-Ringer bicarbonate solution. The tissues were pinned to the base of a Sylgard dish, and the mucosa was removed by sharp dissection. Small strips of intestinal muscle (consisting of both circular and longitudinal muscles) were equilibrated in Ca^{2+}-free Hank's solution (containing 5.36 mM KCl, 125 mM NaCl, 0.34 mM NaOH, 0.44 mM Na_2HCO_3, 10 mM glucose, 2.9 mM sucrose and 11 mM HEPES) for 30 min, and the cells were then dispersed with a solution containing collagenase (Worthington Biochemical Co., Lakewood, NJ, USA) 1.3 mg/mL, bovine serum albumin (Sigma Chemical Co., Saint Louis, MO, USA) 2 mg/mL, trypsin inhibitor (Sigma) 2 mg/mL, and ATP 0.27 mg/mL. The dispersed cells were plated onto sterile glass coverslips coated with murine collagen (2.5 μg/mL, Falcon/BD, Franklin Lakes, NJ, USA) in 35-mm culture dishes and cultured at 37°C in a 95% O_2–5% CO_2 incubator in smooth muscle growth medium (Clonetics Corp., Walkersville, MD, USA) supplemented with 2% antibiotics/antimycotics (Gibco, Grand Island, NY, USA) and murine stem cell factor (5 ng/mL, Sigma). ICCs were identified immunologically by incubation with anti-c-kit antibody (phycoerythrin [PE]-conjugated rat antimouse c-kit monoclonal antibody; eBioscience, La Jolla, CA, USA) at a dilution of 1:50 for 20 min (Goto et al. 2004). Since the morphology of the ICCs differed from those of other cell types in the culture, it was possible to identify them with a phase contrast microscope after incubation with anti-c-kit antibody.

Cells

The most common human gastric adenocarcinoma cell line (AGS) and breast adenocarcinoma cell line (MCF-7) were used. AGS and MCF-7 cells were established at the Cancer Research Center, College of Medicine, Seoul National University, Korea. Cells were propagated in RPMI-1640 medium (Gibco-BRL) supplemented with 10% heat-inactivated fetal bovine serum and 20 μg/mL penicillin and streptomycin in an atmosphere of 5% CO_2 at 37°C.

Patch-clamp experiments

Experiments were performed at room temperature (22–25°C) by using the whole-cell configuration of the patch-clamp technique. Cells were transferred to a small chamber on the stage of an inverted microscope (IX70; Olympus, Japan) and were constantly perfused in a solution containing 2.8 mM KCl, 145 mM NaCl, 2 mM $CaCl_2$, 10 mM glucose, 1.2 mM $MgCl_2$, and 10 mM HEPES, adjusted to pH 7.4 with NaOH. The pipette solution contained 145 mM Cs-glutamate, 8 mM NaCl, 10 mM Cs-2-bis(2-aminophenoxy)-ethane-*N*,*N*,*N*′,*N*′-tetraacetic acid, and 10 mM HEPES-CsOH, adjusted to pH 7.2 with CsOH. An Axopatch I-D (Axon Instruments, Foster City, CA, USA) was used to amplify membrane currents and potentials. For data acquisition and the application of command pulses, pCLAMP software v.9.2 and Digidata 1322A (Axon Instruments) were used. Results were analyzed by using pClamp and Origin software (Microcal Origin version 6.0).

TRPM7 expression in HEK-293 cells

Human embryonic kidney (HEK)-293 cells transfected with the Flag-murine LTRPC7/pCDNA4-TO construct were grown on glass coverslips with Dulbecco's modified Eagle medium supplemented with 10% fetal bovine serum, blasticidin (5 μg/mL), and zeocin (0.4 mg/mL). TRPM7 (LTRPC7) expression was induced by adding 1 μg/mL tetracycline to the culture medium. Whole-cell patch-clamp experiments were performed at 21–25°C, 24 h after induction by using cells grown on glass coverslips. The solutions were the same as those used for recording whole-cell currents in single ICCs.

Ca^{2+}-activated Cl^- channel expression in HEK-293 cells

HEK-293 cells transfected with pEGFP-N1-mANO1 construct were grown on glass coverslips with Dulbecco's modified Eagle medium supplemented with 10% fetal bovine serum. Whole-cell patch-clamp experiments were performed at 21–25°C, 24 h after induction by using cells grown on glass coverslips. The bath solution contained 146 mmol/L HCl, 10 mmol/L HEPES, 10 mmol/L glucose, 1 mmol/L $MgCl_2$, 1 mmol/L $CaCl_2$, and 150 mmol/L *N*-methyl-D-glucamine (NMDG), adjusted to pH 7.4. The pipette solution contained 134 mmol/L HCl, 5 mmol/L HEPES, 10 mmol/L glucose, 1 mmol/L $MgCl_2$, 1 mmol/L $CaCl_2$, and 150 mmol/L NMDG, adjusted to pH 7.2.

MTT assay

Cell viability was assessed by 3-[4,5-dimethylthiazol-2-yl]-2,5-diphenyltetrazolium bromide (MTT) assay. The AGS cells were seeded into each well of 12-well culture plates and then cultured in RPMI-1640 supplemented with other reagents for 24 h. After incubation, 100 μL of MTT solution (5 mg/mL in PBS) was added to each well, and the plates were then incubated for 4 h at 37°C. After removing the supernatant and shaking

with 200 μL of dimethyl sulfoxide (Jersey Lab Supply, Livingston, NJ, USA) for 30 min, absorbance was measured at 570 nm. All experiments were repeated at least three times.

RNA interference

All the synthetic small interfering RNAs (siRNAs) were designed at Qiagen using the BIOPREDsi algorithm licensed from Novartis. All siRNA target sequences for silencing of the *TRPM7* gene (GenBank Accession Number NM_017672) were as follows: TRPM7-siRNA-5′-CCCTGACGGTAGATACATTA A-3′. SiRNA transfections were performed in 12-well plates. Previously, we showed the TRPM7 knock down effects of this TRPM7-specific siRNA (Kim et al. 2008).

Flow cytometric analysis

In order to investigate whether the cell cycle of AGS and MCF-7 cells was redistributed, flow cytometric analysis was used with propidium iodine (PI) stain (Nicoletti et al. 1991; Wang et al. 2005). Cells (1×10^6) were placed in an e-tube and 700 μL of a ice-cold fixation buffer (ethyl alcohol) was slowly added with vortexing. Tubes were sealed with parafilm and incubated at 4°C overnight. Samples were spun for 3 min at 106*g* at 4°C, and the supernatant was aspirated and discarded. The cell pellet was resuspended by 200 μL of PI staining solution (PI [5 mg/mL] 2 μL and RNase 2 μL in PBS 196 μL) at 20,817*g* for 5 s. After 30 min in the dark at room temperature, samples were analyzed in a fluorescence-activated cell sorter (FACScan; Becton-Dickinson, Mountain View, CA, USA) at $\lambda = 488$ nm using Cell-Quest software (Becton-Dickinson). The DNA content distribution of normal growing cells is characterized by two peaks, the G1/G0 and G2/M phases. The G1/G0 phase comprises the normal functioning and resting state of the cell cycle with the most diploid DNA content, while the DNA content in the G2/M phase is more than diploid. Cells in the sub-G1 phase have the least DNA content in cell cycle distribution; this is termed hypodiploid. The hypoploid DNA contents represent the DNA fragmentation (Wang et al. 2005).

Caspase-3 assay

Caspase-3 assay kits (Cellular Activity Assay Kit Plus) were purchased from BioMol (Plymouth, PA, USA). After experimental treatment, cells were centrifuged (1000*g*, 4°C, 10 min) and washed with PBS. Cells were resuspended in ice-cold cell lysis buffer and incubated on ice for 10 min. Sample was centrifuged at 10,000*g* (4°C, 10 min), and the supernatant was removed. Supernatant samples (10 μL) were incubated with 50 μL of substrate (400-μM Ac-DEVD-pNA) in 40 μL of assay buffer at 37°C. Absorbance at 405 nm was read at several time-points. pNA concentration in samples was extrapolated from a standard created with absorbances of sequential pNA concentrations.

Statistical analysis

Data are expressed as mean ± standard error of the mean (SEM). Differences between the data were evaluated by Student's *t*-test. A *P*-value of 0.05 was taken to indicate a statistically significant difference. The *n*-values reported in the text refer to the number of cells used in the patch-clamp experiments.

Results

GTS depolarizes the resting membrane potentials and decreases the amplitude of pacemaker potentials in cultured ICC

The patch-clamp technique was tested on ICC that formed network-like structures in culture (2 4 days). Spontaneous rhythms were routinely recorded from cultured ICC under current- and voltage-clamp conditions, and the ICC within networks displayed more robust electrical rhythms. Tissue-like spontaneous slow waves have been recorded from these cells (Koh et al. 1998). To understand the relationship between GTS and the modulation of pacemaker activity in ICC, we examined the effects of GTS on pacemaker potentials. In current-clamp mode (I = 0), ICC had a mean resting membrane potential of -53 ± 2 mV and produced electrical pacemaker potentials ($n = 25$). The frequency of this pacemaker potential was 17 ± 1 cycles/min with an amplitude of 33 ± 3 mV ($n = 25$). The addition of GTS (1–10 μg/mL) decreased the amplitude of the pacemaker potentials and depolarized the resting membrane potentials (Figure 1). The amplitudes were 33.1 ± 3 mV at 1 μg/mL GTS, 15.2 ± 4 mV at 5 μg/mL GTS, and 5.3 ± 2 mV at 10 μg/mL GTS ($n = 5$; Figure 1B). The corresponding resting membrane depolarizations were 14.1 ± 2, 20.2 ± 4.1 and 30.1 ± 3.3 mV ($n = 5$; Figure 1C).

Effects of GTS on the TRPM7-like currents in ICC and the overexpressed TRPM7 or Ca^{2+}-activated Cl^- currents in HEK293 cells

We previously suggested that TRPM7 is required for pacemaker activity in ICCs (Kim et al. 2005) and found that GTS modulated the pacemaker activity in ICCs. Therefore, we investigated the role of GTS in TRPM7

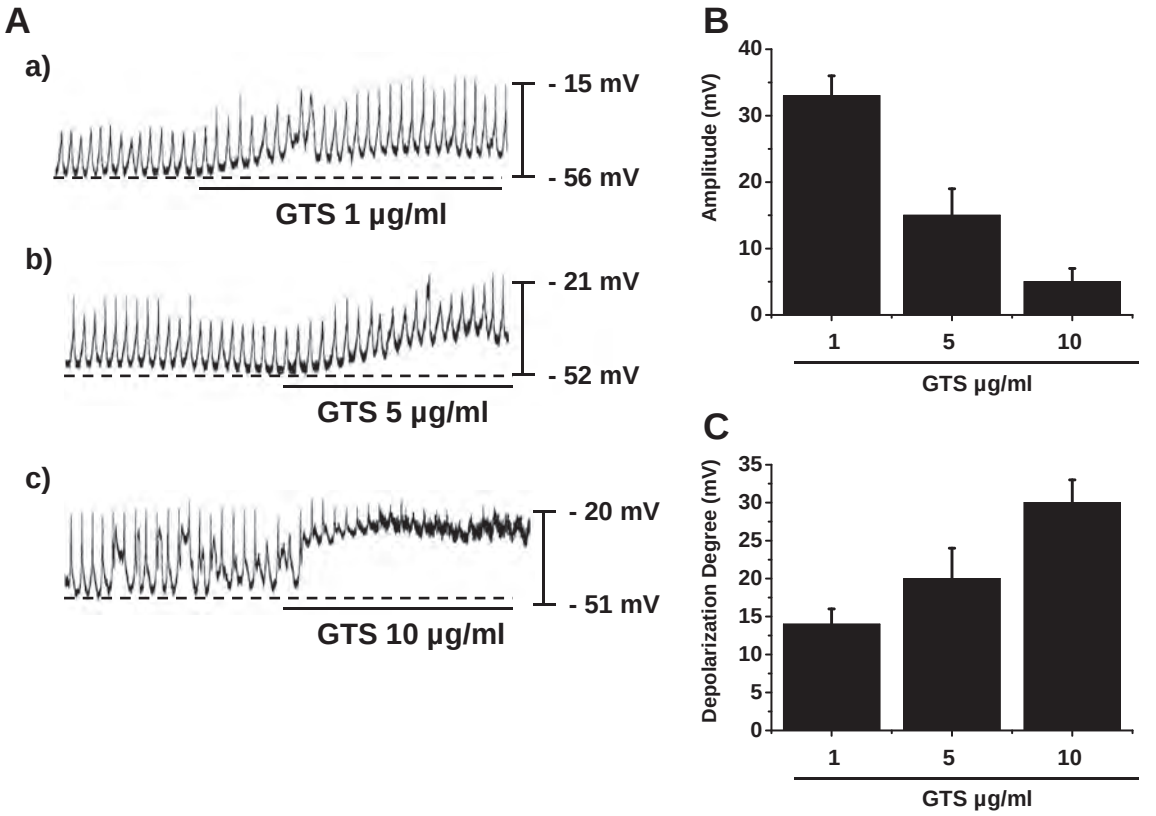

Figure 1. GTS decreases the amplitude of pacemaker potentials in cultured ICCs. (A) In current-clamp mode (I = 0), the addition of GTS (1–10 μg/mL) decreases the amplitude of pacemaker potentials and depolarized resting membrane potentials. (B) The histograms summarize the decrease of amplitude with GTS concentration. (C) The histograms summarize the depolarization of resting membrane potentials with GTS concentration.

channels. To record the TRPM7-like current involved in pacemaking activity, we performed whole-cell voltage-clamp recordings in cultured single ICCs. Single ICCs were identified with PE-bound anti-c-kit antibody. A voltage ramp from -100 to $+100$ mV evoked an outward-rectifying cation current at positive potentials with standard bath solution and with pipette solutions lacking magnesium adenosine triphosphate (Figure 2A). These features are very similar to those associated with the recently cloned TRPM7 channel (Nadler et al. 2001). The TRPM7-like currents in single ICCs were recorded, and these currents were inhibited by GTS 10 μg/mL ($n = 5$; Figure 2A). Similar results were obtained in HEK cells overexpressing TRPM7 ($n = 5$; Figure 2B). However, recently, Zhu et al. (2009) suggested that Ca^{2+}-activated Cl^- conductance is involved in pacemaking activity in ICCs, and a recent study confirmed that ICC expresses ANO1 in the GI tract (Gomez-Pinilla et al. 2009). ANO1 was recently shown to function as a Ca^{2+}-activated Cl channel (Schroeder et al. 2008; Yang et al. 2008), and loss or block of ANO1 blocks electrical slow waves in intact GI muscles (Hwang et al. 2009). Therefore, we investigated the effect of GTS in Ca^{2+}-activated Cl^- conductance. We overexpressed Ca^{2+}-activated Cl^- channels in HEK293 cells. Whole cell currents were recorded using patch-clamp techniques. To determine the current–voltage (I–V) relationship, we applied a ramp pulse from -100 to $+100$ mV for 2 s. However, GTS had no effect on Ca^{2+}-activated Cl^- conductance (Figure 2C).

Cell death by GTS in AGS and MCF-7 cells

Functional TRPM7 channels are expressed in AGS cells where they play important roles in cell death (Kim et al. 2008). Also, TRPM7 is involved in the proliferative potentiality of breast cancer MCF-7 cells (Guilbert et al. 2009). However, whether TRPM7 channels play a role in GTS-mediated cytotoxicity in AGS and MCF-7 cells has never been explored. Therefore, we investigated whether the GTS influences the survival of AGS and MCF-7 cells. First, we tested the effect of GTS on the survival of AGS cells. Addition of 10 μg/mL GTS in the culture medium inhibited the survival of AGS cells by $68.1 \pm 5.1\%$ with MTT assay ($n = 4$; Figure 3A). To investigate electrophysiological characteristics in AGS cells, we

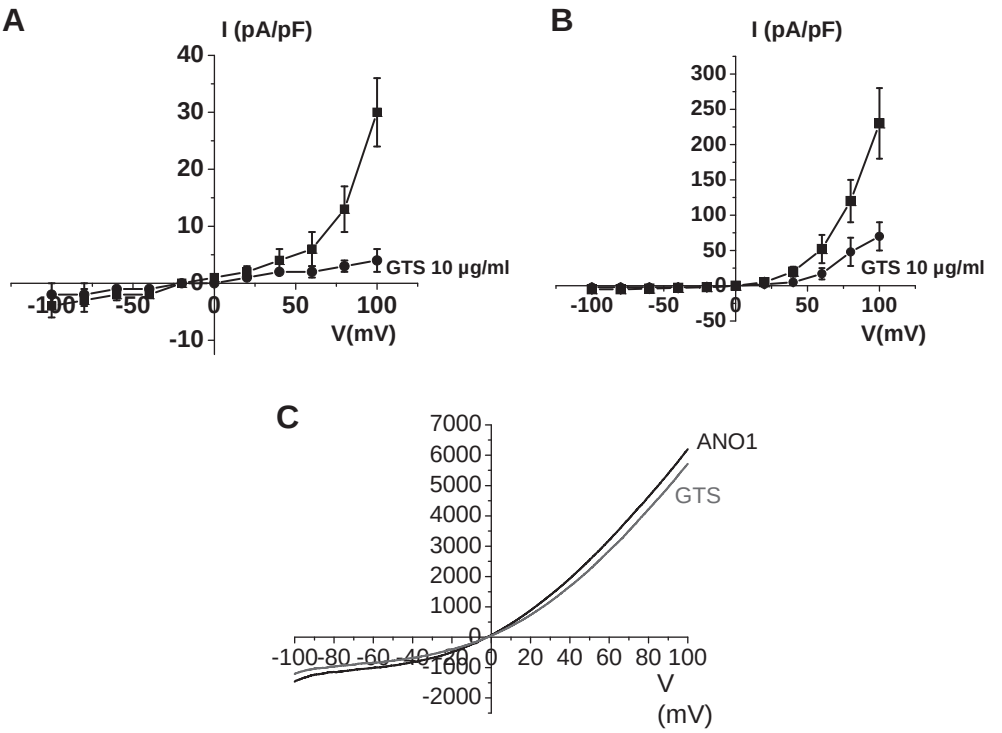

Figure 2. Effects of GTS on the TRPM7-like currents in ICC and the overexpressed TRPM7 or Ca^{2+}-activated Cl^- currents in HEK293 cells. (A) Representative TRPM7-like currents in ICCs. A voltage ramp from –100 to +100 mV was applied from a holding potential of −60 mV. A single ICC was identified with PE-bound anti-c-kit antibody. (B) Current–voltage relationships for expressed TRPM7 in HEK293 cells. A voltage ramp from −100 to +100 mV was applied from a holding potential of −60 mV. (C) Representative I–V relationships of the effect of GTS on Ca^{2+}-activated Cl^- currents in HEK293 cells. GTS had no effect on the currents. A voltage ramp from +100 to −100 mV was applied from a holding potential of −60 mV.

performed whole-cell voltage-clamp recordings. A voltage ramp from −100 to +100 mV evoked small inward currents at negative potentials, whereas larger outward currents were evoked at positive potentials, showing outward-rectifying cation currents ($n = 6$; Figure 3B). In the presence of 10 μg/mL GTS, the amplitude of the currents was inhibited by $62.8 \pm 2.1\%$ outwardly and $87.1 \pm 3.2\%$ inwardly ($n = 6$; Figure 3B). Next, we tested the effect of GTS on the survival of MCF-7 cells. Addition of 10 μg/mL GTS in the culture medium inhibited the survival of MCF-7 cells by $74.2 \pm 4.3\%$ with MTT assay ($n = 4$; Figure 3C). To investigate electrophysiological characteristics in MCF-7 cells, we performed whole-cell voltage-clamp recordings. A voltage ramp from −100 to +100 mV evoked small inward currents at negative potentials, whereas larger outward currents were evoked at positive potentials, showing outward-rectifying cation currents ($n = 6$; Figure 3D). In the presence of 10 μg/mL GTS, the amplitude of the currents was inhibited by $63.9 \pm 1.2\%$ outwardly and $89.1 \pm 1.3\%$ inwardly ($n = 6$; Figure 3D). For determination that these effects were really mediated by activation of TRPM7 channels, we used RNA interference. Previously, we created the 21-nucleotide siRNA specifically targeting human TRPM7 (Kim et al. 2008). Depletion of TRPM7 in AGS and MCF-7 cells rendered the cells more resistant to GTS. In the presence of 10 μg/mL GTS, the cell death was attenuated by $34.3 \pm 1.2\%$ in AGS and $38.1 \pm 2.3\%$ in MCF-7 cells in TRPM7siRNA with the MTT assay ($n = 4$; Figure 4). Taken together, these data indicate that TRPM7 channels are involved in GTS-mediated cell death in AGS and MCF-7 cells.

Cell death by GTS leads to increased apoptosis

To determine whether AGS and MCF-7 cell death occurred by apoptosis, we used sub-G1 analysis and caspase-3 activity. As a method to analyze the mode of cell death in AGS and MCF-7 cells by GTS, we used sub-G1 analysis (Hotz et al. 1994; Vermes et al. 2000). In this protocol, AGS and MCF-7 cells with GTS are stained with a fluorescent DNA stain (such as PI). Due to the action of endogenous endonucleases in apoptotic cells, the DNA is cleaved into endonucleosomal fragments of typical sizes. These DNA fragments are extracted from the cells. This loss of DNA is detectable by FACS analysis, as the reduced nuclear staining of

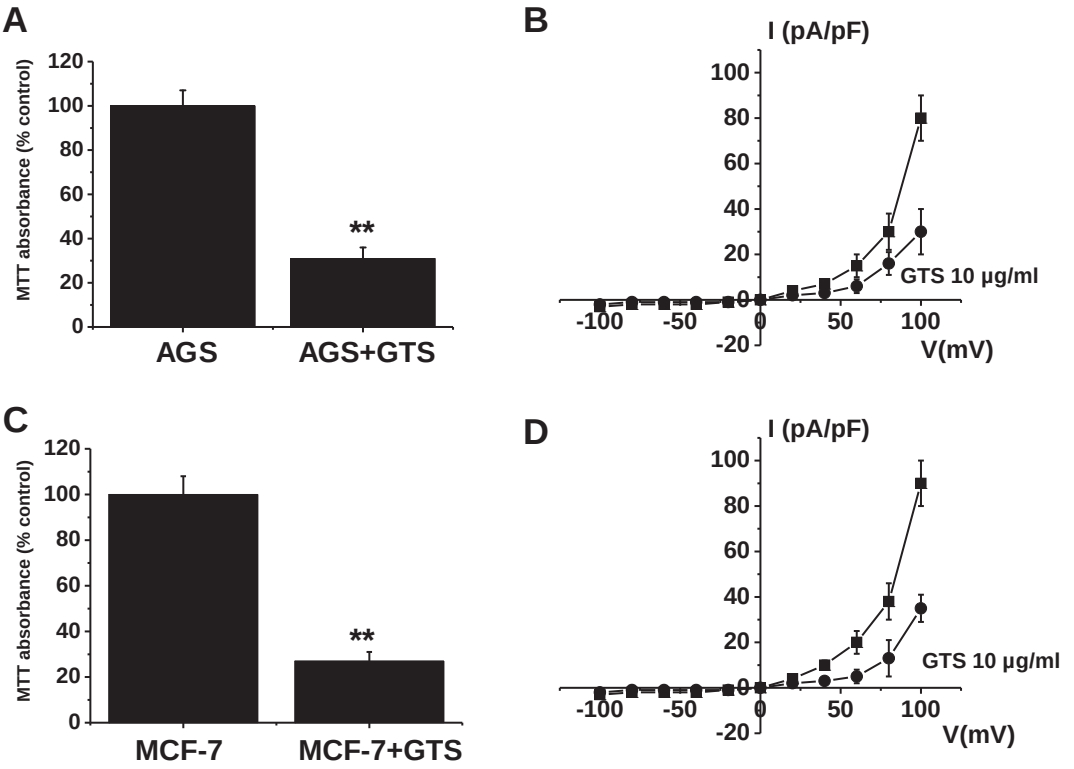

Figure 3. Effect of GTS on cell viability with an MTT-based viability assay in AGS and MCF-7 cells. (A) Cell viability was significantly decreased by GTS in AGS cells. (B) GTS inhibited the TRPM7-like current in AGS cells. (C) Cell viability was significantly decreased by GTS in MCF-7 cells. (B) GTS inhibited the TRPM7-like current in MCF-7 cells. Values are mean $\pm$ SEM. $^{*}P < 0.05$, $^{**}P < 0.01$.

apoptotic cells results in a novel (sub-G1) fluorescence peak to the left of the regular fluorescence peak. The sub-G1 in AGS cells with GTS was markedly increased by $14.3 \pm 1.2\%$ (Figure 5A). And the sub-G1 in MCF-7 cells with GTS was markedly increased by $17.5 \pm 2.3\%$ (Figure 5C). Caspase-3 activation is one of the hallmarks of apoptotic cell death (Faleiro et al. 1997; Kang 2008; Jang et al. 2009). We measured the enzyme activity in AGS and MCF-7 cells with GTS. In AGS and MCF-7 cells with GTS, caspase-3 activity was increased approximately 1.5-fold (Figure 5B and D).

Discussion

Ginsenosides, the active ingredients of *P. ginseng*, have been widely used as invigorating agents, and many reports have described a variety of physiological and pharmacological effects in various organs and tissues (Attele et al. 1999). Ginsenosides have an important role in ion channels. Ginsenoside-Rd attenuated TRPM7 and acid-sensing ion channels 1a expression in rats after focal cerebral ischemia (Zhang et al. 2012) and GTS and ginsenoside Rg3 increased the large conductance K (Ca) channel (Sung et al. 2011). Ginsenoside Rg3 decelerated hERG K+ channel deactivation through Ser631 residue interaction (Choi, Shin, Hwang, et al. 2011; Choi, Shin, Lee, et al. 2011) and enhanced large conductance Ca2+-activated potassium channel currents through Tyr360 residue (Choi, Shin, Hwang, et al. 2011; Choi, Shin, Lee, et al. 2011). Also Rg3-activated human KCNQ1 K+ channel currents through interacting with the K318 and V319 residues (Choi et al. 2010). Alpha7 nicotinic acetylcholine receptor was regulated by ginsenoside through a role for Leu247 residue within transmembrane domain 2 (Lee, Choi, Pyo, et al. 2009; Lee, Choi, Lee, et al. 2009) and human Kv1.4 channel currents were regulated by Rg3 without the N-terminal rapid inactivation (Lee, Choi, Pyo, et al. 2009; Lee, Choi, Lee, et al. 2009). However, there are only a few reports on the effects of ginsenosides on TRP channels.

In this study, we provided evidence suggesting that TRPM7 is an important player for GTS-induced cytotoxicity. (1) GTS modulated intestinal motility by modulating the pacemaker potentials of ICCs (Figure 1). (2) GTS blocked the TRPM7-like current in single ICC and the overexpressed TRPM7 currents in HEK 293 cells (Figure 2). (3) MTT assay revealed that addition of GTS induced the death of AGS and

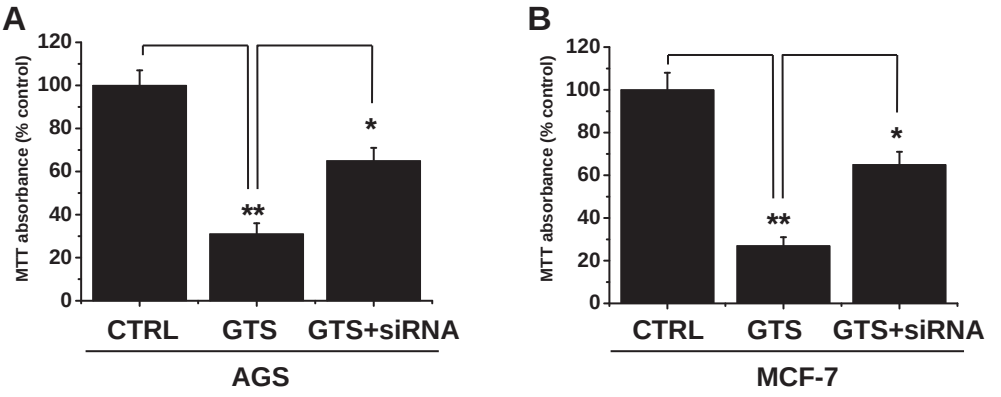

Figure 4. Effect of GTS on cell viability with an MTT-based viability assay in AGS and MCF-7 cells. (A) and (B) Cell viability was significantly decreased by GTS. However, inhibition of TRPM7 channels by siRNA reduced GTS toxicity. Values are mean ± SEM. siRNA, TRPM7-specific siRNA. $*P < 0.05$, $**P < 0.01$.

MCF-7 cells. Also by patch-clamp method, the TRPM7-like currents in AGS and MCF-7 cells were inhibited by GTS (Figure 3). (4) The presence of TRPM7 specific siRNA attenuated the death of AGS and MCF-7 cells (Figure 4). (5) By FACScan and caspase-3 activity, GTS-mediated cell damages were apoptotic processes (Figure 5).

We demonstrated that TRPM7 has an important role in the pacemaking activity of ICCs (Kim et al. 2005), and human gastric adenocarcinoma cells express functional TRPM7 channels that are involved in cell growth and survival (Kim et al. 2008). Also, TRPM7 channel could regulate the proliferation of human breast cancer cells (Guilbert et al. 2009).

Therefore, we first investigated the effect of GTS in ICCs and then the involvement of TRPM7 channels in GTS-mediated cell death in AGS and MCF-7 cells. In AGS and MCF-7 cells, TRPM7 channels have an

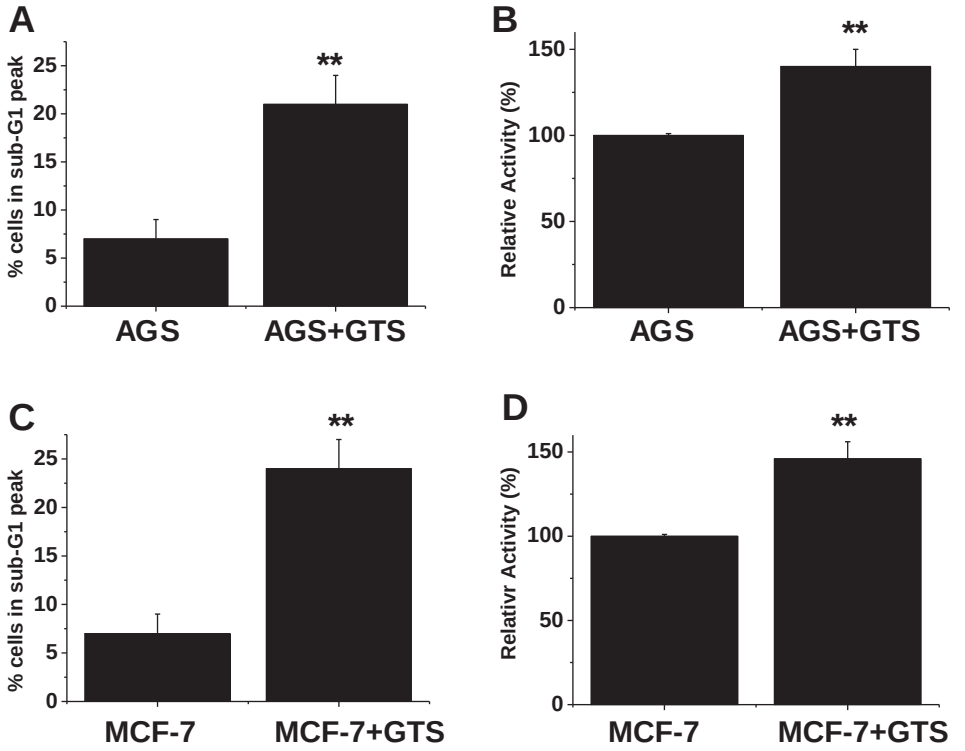

Figure 5. Cell death by GTS lead to increased apoptosis. (A) and (C) Sub-G1 peak measured by FACScan. In the presence of GTS, the sub-G1 in AGS and MCF-7 cells was decreased. Quantitative data of three independent experiments. (B) and (D) Caspase-3 activities measured by enzyme assays. In the presence of GTS, caspase-3 activity decreased. The specific activity was obtained from three samples per group. $*P < 0.05$, $**P < 0.01$.

important role in GTS-induced cell death and are inhibited by GTS. However, the cellular mechanisms in GTS-mediated cell death require more investigation. In future, the Bcl-2/Bax ratio, the change of cytochrome-*c* from mitochondria, or the involvement of other channels will be good themes to explore.

In summary, we have demonstrated that functional TRPM7 channels are involved, at least partially, in GTS-mediated cell survival in human gastric and breast adenocarcinoma cells.

Acknowledgements

This research was supported by Basic Science Research Program through the National Research Foundation of Korea and funded by the Ministry of Education, Science and Technology (2010-0021347).

References

Attele AS, Wu JA, Yuan CS. 1999. Ginseng pharmacology: multiple constituents and multiple actions. Biochem Pharmacol. 58:1685–1693.

Choi SH, Shin TJ, Lee BH, Chu DH, Choe H, Pyo MK, Hwang SH, Kim BR, Lee SM, Lee JH, et al. 2010. Ginsenoside Rg3 activates human KCNQ1 K+ channel currents through interacting with the K318 and V319 residues: a role of KCNE1 subunit. Eur J Pharmacol. 637:138–147.

Choi SH, Shin TJ, Hwang SH, Lee BH, Kang J, Kim HJ, Jo SH, Choe H, Nah SY. 2011. Ginsenoside Rg(3) decelerates hERG K(+) channel deactivation through Ser631 residue interaction. Eur J Pharmacol. 663:59–67.

Choi SH, Shin TJ, Lee BH, Hwang SH, Lee SM, Lee BC, Park CS, Ha TS, Nah SY. 2011. Ginsenoside Rg3 enhances large conductance Ca2 + -activated potassium channel currents: a role of Tyr360 residue. Mol Cells 31:133–140.

Clapham DE. 2003. TRP channels as cellular sensors. Nature 426:517–524.

Faleiro L, Kobayashi R, Fearnhead H, Lazebnik Y. 1997. Multiple species of CPP32 and Mch2 are the major active caspases present in apoptotic cells. EMBO J. 16:2271–2281.

Gomez-Pinilla PJ, Gibbons SJ, Bardsley MR, Lorincz A, Pozo MJ, Pasricha PJ, Van de Rijn M, West RB, Sarr MG, Kendrick ML, et al. 2009. Ano1 is a selective marker of interstitial cells of Cajal in the human and mouse gastrointestinal tract. Am J Physiol Gastrointest Liver Physiol. 296:G1370–G1381.

Goto K, Matsuoka S, Noma A. 2004. Two types of spontaneous depolarizations in the interstitial cells freshly prepared from the murine small intestine. J Physiol. 559:411–422.

Guilbert A, Gautier M, Dhennin-Duthille I, Haren N, Sevestre H, Ouadid-Ahidouch H. 2009. Evidence that TRPM7 is required for breast cancer cell proliferation. Am J Physiol Cell Physiol. 297:C493–C502.

Hotz MA, Gong J, Traganos F, Darzynkiewicz Z. 1994. Flow cytometric detection of apoptosis: comparison of the assays of in situ DNA degradation and chromatin changes. Cytometry 15:237–244.

Hwang SJ, Blair PJA, Britton FC, O'Driscoll KE, Hennig G, Bayguinov YR, Rock JR, Harfe BD, Sanders KM, Ward SM. 2009. Expression of anoctamin 1/TMEM16A by interstitial cells of Cajal is fundamental for slow wave activity in gastrointestinal muscles. J Physiol. 587:4887–4904.

Jang SM, Kim JW, Choi KH. 2009. p19ras accelerates p73β-mediated apoptosis through a caspase-3 dependent pathway. Anim Cells Syst. 13:399–403.

Jiang J, Li MH, Inoue K, Chu XP, Seeds J, Xiong ZG. 2007. Transient receptor potential melastatin 7-like current in human head and neck carcinoma cells: role in cell proliferation. Cancer Res. 67:10929–10938.

Jin J, Desai BN, Navarro B, Donovan A, Andrews NC, Clapham DE. 2008. Deletion of Trpm7 disrupts embryonic development and thymopoiesis without altering Mg^{2+} homeostasis. Science 322:756–760.

Kang SJ. 2008. A possible physiological role of caspase-11 during germinal center reaction. Anim. Cells Syst. 12:127–136.

Kim BJ, Lim HH, Yang DK, Jun JY, Chang IY, Park CS, So I, Stanfield PR, Kim KW. 2005. Melastatin-type transient receptor potential channel 7 is required for intestinal pacemaking activity. Gastroenterology 129:1504–1517.

Kim BJ, Park EJ, Lee JH, Jeon JH, Kim SJ, So I. 2008. Suppression of transient receptor potential melastatin 7 channel induces cell death in gastric cancer. Cancer Sci. 99:2502–2509.

Kim S, Ahn K, Oh TH, Nah SY, Rhim H. 2002. Inhibitory effect of ginsenosides on NMDA receptor-mediated signals in rat hippocampal neurons. Biochem Biophys Res Commun. 296:247–254.

Kim S, Kim T, Ahn K, Park WK, Nah SY, Rhim H. 2004. Ginsenoside Rg3 antagonizes NMDA receptors through a glycine modulatory site in rat cultured hippocampal neurons. Biochem Biophys Res Commun. 323:416–424.

Koh SD, Sanders KM, Ward SM. 1998. Spontaneous electrical rhythmicity in cultured interstitial cells of cajal from the murine small intestine. J Physiol. 513:203–213.

Lee BH, Choi SH, Pyo MK, Shin TJ, Hwang SH, Kim BR, Lee SM, Lee JH, Lee JH, Lee HS, et al. 2009. A role for Leu247 residue within transmembrane domain 2 in ginsenoside-mediated alpha7 nicotinic acetylcholine receptor regulation. Mol Cells. 27:591–599.

Lee JH, Choi SH, Lee BH, Shin TJ, Pyo MK, Hwang SH, Kim BR, Lee SM, Bae DH, Rhim H, Nah SY. 2009. The effects of ginsenoside Rg(3) on human Kv1.4 channel currents without the N-terminal rapid inactivation domain. Biol Pharm Bull. 32:614–618.

Nadler MJ, Hermosura MC, Inabe K, Perraud AL, Zhu Q, Stokes AJ, Kurosaki T, Kinet JP, Penner R, Scharenberg AM, et al. 2001. LTRPC7 is a Mg.ATP-regulated divalent cation channel required for cell viability. Nature 411:590–595.

Nah SY. 1997. Ginseng: recent advances and trends. Korea J Ginseng Sci. 21:1–12.

Nicoletti I, Migliorati G, Pagliacci MC, Grignani F, Riccardi C. 1991. A rapid and simple method for measuring thymocyte apoptosis by propidium iodide staining and flow cytometry. J Immunol Methods 139:271–279.

Rhim H, Kim H, Lee DY, Oh TH, Nah SY. 2002. Ginseng and ginsenoside Rg3, a newly identified active ingredient of ginseng, modulate Ca2+ channel currents in rat sensory neurons. Eur J Pharmacol. 436:151–158.

Schmitz C, Perraud AL, Johnson CO, Inabe K, Smith MK, Penner R, Kurosaki T, Fleig A, Scharenberg AM. 2003. Regulation of vertebrate cellular Mg^{2+} homeostasis by TRPM7. Cell 114:191–200.

Schroeder BC, Cheng T, Jan YN, Jan LY. 2008. Expression cloning of TMEM16A as a calcium-activated chloride channel subunit. Cell 134:1019–1029.

Sung HH, Chae MR, So I, Jeon JH, Park JK, Lee SW. 2011. Effects of ginsenoside on large-conductance K(Ca) channels in human corporal smooth muscle cells. Int J Impot Res. 23:193–199.

Vermes I, Haanen C, Reutelingsperger C. 2000. Flow cytometry of apoptotic cell death. J Immunol Methods 243:167–190.

Wang BJ, Won SJ, Yu ZR, Su CL. 2005. Free radical scavenging and apoptotic effects of cordycepin sinensis ractionated by supercritical carbon dioxide. Food Chem Toxicol. 43:543–552.

Yang YD, Cho H, Koo JY, Tak MH, Cho Y, Shim WS, Park SP, Lee J, Lee B, Kim BM, et al. 2008. TMEM16A confers receptor-activated calcium-dependent chloride conductance. Nature 455:1210–1215.

Zhang Y, Zhou L, Zhang X, Bai J, Shi M, Zhao G. 2012. Ginsenoside-Rd attenuates TRPM7 and ASIC1a but promotes ASIC2a expression in rats after focal cerebral ischemia. Neurol Sci.

Zhu MH, Kim TW, Ro S, Yan W, Ward SM, Koh SD, Sanders KM. 2009. A Ca(2 +)-activated Cl(−) conductance in interstitial cells of Cajal linked to slow wave currents and pacemaker activity. J Physiol. 587:4905–4982.